12-1997

Temporal and spatial variability of snow accumulation in central Greenland

H Kuhns
Desert Research Inst.

C Davidson
Carnegie Mellon University

Jack E. Dibb
University of New Hampshire, jack.dibb@unh.edu

C Stearns
University of Wisconsin-Madison

M H. Bergin
University of Colorado, Boulder

See next page for additional authors

Recommended Citation

Kuhns, H., C. Davidson, J. Dibb, C. Stearns, M. Bergin, and J.-L. Jaffrezo (1997), Temporal and spatial variability of snow accumulation in central Greenland, J. Geophys. Res., 102(D25), 30059–30068, doi:10.1029/97JD02760.

JOURNAL OF GEOPHYSICAL RESEARCH, VOL. 102, NO. D25, PAGES 30,059–30,068, DECEMBER 27, 1997

Temporal and spatial variability of snow accumulation in central Greenland

H. Kuhns,[1] C. Davidson,[2] J. Dibb,[3] C. Stearns,[4] M. Bergin,[5,6] and J.-L. Jaffrezo[7]

Abstract. Snow accumulation records from central Greenland are explored to improve the understanding of the accumulation signal in Greenland ice core records. Results from a "forest" of 100 bamboo poles and automated accumulation monitors in the vicinity of Summit as well as shallow cores collected in the Summit and Crete areas are presented. Based on these accumulation data, a regression has been calculated to quantify the signal-to-noise variance ratio of ice core accumulation signals on a variety of temporal (1 week to 2 years) and spatial (20 m to 200 km) scales. Results are consistent with data obtained from year-round automated accumulation measurements deployed at Summit which suggest that it is impossible to obtain regional snow accumulation data with seasonal resolution using four accumulation monitors positioned over a length scale of ~30 km. Given this understanding of the temporal and spatial dependence of noise in the ice core accumulation signal, the accumulation records from 17 shallow cores are revisited. Each core spans the time period from 1964 to 1983. By combining the accumulation records, the regional snow accumulation record has been obtained for this period. The results show that 9 of the 20 years can be identified as having an accumulation different from the 20 year mean with 99% confidence. The signal-to-noise variance ratio for the average accumulation signal sampled at annual intervals is 5.8 ± 0.5. The averaged accumulation time series may be useful to climate modelers attempting to validate their models with accurate regional hydrologic data sets.

1. Introduction

The Summit, Greenland Atmospheric Sampling Program (ATM) originated in 1989 in conjunction with the retrieval of the 3000 m Greenland Ice Sheet Project (GISP2) ice core [*Dibb and Jaffrezo*, 1997; *Jaffrezo et al.*, 1995]. The program has continued through the 1996 summer season. A primary objective of the program is to quantify relations between chemical species concentrations in the air and those in the snow to improve our understanding of chemical variations in ice core records. To achieve this objective, experiments have been carried out every summer to measure atmospheric concentrations, deposition fluxes, and surface snow concentrations of the same chemical species often measured in ice cores. In addition, measurements of the accumulation of snow have been conducted.

[1]Energy and Environmental Engineering Center, Desert Research Institute, Las Vegas, Nevada.
[2]Dept. of Civil and Environmental Engineering, Carnegie Mellon University, Pittsburgh, Pennsylvania.
[3]Institute for the Study of Earth, Oceans, and Space, University of New Hampshire, Durham, New Hampshire.
[4]Dept. of Atmospheric and Oceanic Sciences, University of Wisconsin, Madison, Wisconsin.
[5]Climate Modeling and Diagnostic Laboratory, National Oceanographic and Atmospheric Administration, Boulder, Colorado.
[6]Also at Environmental Chemistry Division, Brookhaven National Laboratory, Upton, New York.
[7]Laboratoire de Glaciologie et Géophysique de l'Environment, Domaine Universitaire, Grenoble, France.

Paper number 97JD02760.
0148-0227/97/97JD-02760$09.00

Since most chemical species in ice cores are determined as grams of impurity per gram of water, understanding the rates of accumulation of snow on the ice sheet is fundamental to the primary objective of the overall program. The relationship between accumulation and concentration in snow pit records was explored by *Mayewski et al.* [1990]. Their results showed that for sulfate and nitrate there may be a slight inverse relationship between impurity concentrations in snow pits and the accumulation rate. Consequently, it is important to understand the relationship between the accumulation estimated from a single ice core and the regional snow accumulation.

Several studies to date have addressed some of the complexities of snow accumulation on the Greenland Ice Sheet. Spatial variations have been explored by *Clausen et al.* [1988] and *Bolzan and Strobel* [1994]. These authors have collected numerous ice cores within 200 km of Summit and mapped the average annual snow accumulation in this area. Their results show that the mean annual accumulation rate can vary by a factor of 2 over this region. Figure 1 shows the location of the Bolzan and Clausen coring sites as well as the locations of the stations at which other data in this paper were collected.

Temporal trends have been studied by *Bromwich et al.* [1993], who used geopotential height fields between 1963 and 1988 to simulate the interannual and intraannual variations of precipitation distributed over the entire Greenland Ice Sheet. Their model indicated that more snowfall is expected in the summer than in the winter.

In the present work, multiple types of accumulation records are combined to generate a regression that relates the correlation between two ice core accumulation records to the horizontal spacing of the cores and the temporal sampling of

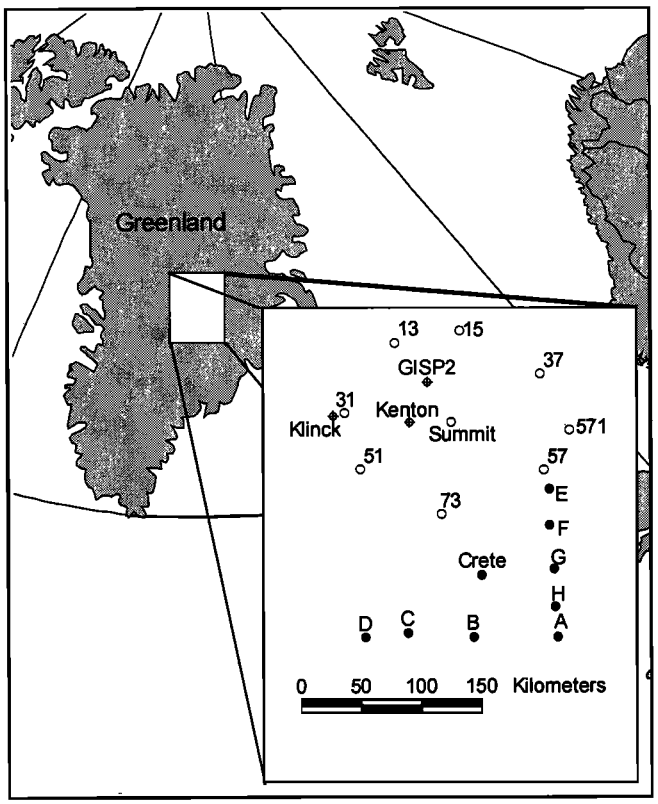

Figure 1. Map of the Summit area on the Greenland Crest showing the locations of Summit, GISP2 AWS and ADG, Kenton ADG and bamboo forest, Klink ADG, Bolzan accumulation survey [*Bolzan and Strobel*, 1994], and Clausen survey [*Clausen et al.*, 1988].

the record. The regression quantitatively characterizes the spatial variability of snow accumulation and should guide the design of future coring experiments that will produce statistically significant regional accumulation records. Moreover, by determining the spatial and temporal dependence of the correlation between two ice cores, we will be able to estimate what fraction of the accumulation signal from a single ice core is due to a regional accumulation signal and what fraction is simply spatial noise.

2. Experimental Methods

Three types of snow accumulation measurements were employed in the vicinity of ATM, Greenland (72.58°N, 38.46°W, 3205 m above see level (asl)). These included manual readings using bamboo poles positioned in the snow, acoustic depth gauges (ADGs), and a vertical thermocouple array (TCA). The last two methods were automated and provided data over the winter when the camp was unmanned (Figure 1).

2.1. Bamboo Forest

Snow accumulation was measured using a "forest" of bamboo poles at the remote air sampling site 28 km SW of the GISP2 ice core drilling camp. An array of 100 poles was erected on a 90 m x 90 m grid with 10 m spacing between each pole. The forest was assembled on August 30, 1990, using poles roughly 3 m high. The poles were raised on August 23, 1991, and again on August 10, 1992. The height of a reference mark on the pole above the snow was measured by a field assistant using a measuring stick with 0.5 cm precision. Accumulation was estimated as the difference in sequential reference height measurements. On May 27, 1995, the top of the pole was used as the measurement reference since the tape on some of the poles had been buried under the snow. One bamboo pole fell over in 1991, and the record of accumulation for that pole was deleted from the data set.

The forest data set spans the dates from August 30, 1990, to July 13, 1995. The number of readings per year was 1 in 1990, 16 in 1991, 14 in 1992, 16 in 1993, 5 in 1994, and 6 in 1995 for a total of 5742 measurements. The individual snow fluxes at each of the poles were compared with the estimated 99.9% confidence intervals of the fluxes at the remaining poles for that time interval. If the flux was outside of the confidence interval, it was assumed that the reading was erroneous (e.g., through misreading the height on the measurement pole by the field assistant), and the individual accumulation measurement was removed from the data set. Of the 5742 accumulation measurements obtained over the 6 year interval, a total of 5372 data points remained. This data filtering method was employed in order to systematically discard obviously erroneous data points that could degrade the following statistical analysis.

A similar accumulation forest at Dome C in East Antarctica using poles spaced at ~3 m effectively collected drifting snow causing the accumulation measurements to be positively biased by as much as a factor of 2 [*Palais,* 1980]. Over the 6 years of measurements at the ATM accumulation forest, no visible enhancement in accumulation was observed between the forest and the surrounding snow surface. While this is not conclusive evidence that the measurements at the ATM forest did not record a positively biased signal, in the following analysis it is assumed that the snow surface was undisturbed by the bamboo poles.

2.2. Acoustic Depth Gauges

Campbell Scientific ADGs were mounted on a tower above the snow surface and used to record the distance from a sound source to the snow surface by reflecting sound waves off the snow. A Campbell Scientific CR10XT was used to record the time, distance to the snow surface, and air temperature at 1 hour intervals. The data were stored on a Campbell Scientific SM192 storage module. During the winter months, when temperatures dropped below -55°C, the ADGs did not function properly and hence these results have been excluded from the ADG data set.

In the 1994 summer field season, three ADGs were deployed on the GISP2 automated weather station (AWS) (72.58°N, 38.46°W, 3205 m asl), the Kenton AWS (72.28°N, 38.82°W, 3185 m asl), and the Klinck AWS (72.31°N, 40.48°W, 3105 m asl). In 1995, the ADG at Klinck was removed from the field.

2.3. Thermocouple Array

An array of 25 thermocouples spanning 75 cm was suspended vertically above the snow surface using a PVC frame and monofilament line. As the snow fell, it buried each successive thermocouple. When a thermocouple was above the snow surface, it measured the ambient air temperature.

However, when buried, the insulating properties of the snow significantly dampened the air temperature fluctuations, and it was possible to determine which thermocouples were buried based on the variance of the diurnal temperature of each thermocouple. Thermocouple spacing was determined by excavating the array after each year of deployment and measuring the depths of the thermocouples with a meter stick.

Data were recorded using a Campbell Scientific CR10XT and an AM25T solid state thermocouple multiplexer. In 1994 the thermocouple array (TCA) was installed approximately 100 m from the GISP2 ADG. In 1995 the thermocouple string was moved to the Kenton site. The distance between the TCA and the Kenton ADG was approximately 100 m.

3. Results and Discussion

3.1. Bamboo Forest

The accumulation data at time t from the bamboo forest are recorded as tape or pole heights $H_{t,i}$ where the subscript i denotes the particular bamboo pole in the array. The changes in those heights between measurements are used to calculate snow accumulation. In order to normalize the data set, the assumption is made that the snow has accumulated around a horizontal plane such that

$$A_{t,j,k} = D_t - H_{t,j,k} \quad (1)$$

where D_i is the distance from the tape to the horizontal plane at time t_0 The subscripts j and k represent the year of the measurement and the measurement number of that year, respectively. $A_{t,j,k}$ is the accumulation at pole i with respect to the horizontal plane since September 30, 1990. That is, the average of all $A_{i,1990,1} = 0$. The offset D_t was numerically calculated by minimizing the cumulative variances of $A_{j,k}$ over the entire 6 year accumulation record. The minimization function was weighted such that each year contributed equally to the cumulative variance. The minimization function used was

$$\min_{D_t}\left[\sum_{j=1990}^{1995}\frac{1}{N_j}\sum_{k=1}^{N_k}\mathrm{Var}(A_{j,k})\right] \quad (2)$$

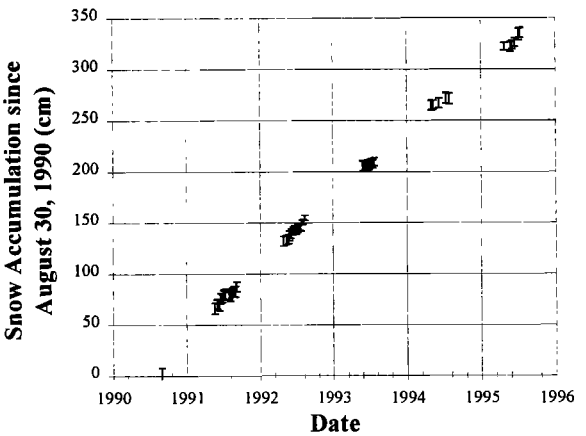

Figure 2. Snow accumulation record from 100 pole bamboo forest at ATM, Greenland. The error bars in this figure represent the standard deviation of the snow surface from a common horizontal reference plane.

where N_j is the number of forest measurements taken in year j, and $\mathrm{Var}(A_{j,k})$ is the variance of $A_{j,k,i}$ over all poles i.

Figure 2 is the time series plot of the mean snow accumulation $\overline{A_{j,k}}$ from the bamboo forest between 1990 and 1995. No correction has been made to this data set to account for the compaction of snow due to drifting or metamorphism. Over this period, the snow accumulation rate remained constant at 65 cm of snow per year. For each accumulation data point $A_{i,j,k}$, the deviation of the snow surface $\varepsilon_{i,j,k}$ from a horizontal plane level with the mean accumulation of the snow surface has been calculated as

$$\varepsilon_{t,j,k} = A_{t,j,k} - \overline{A_{j,k}} \quad (3)$$

The error bars in Figure 2 represent the standard deviation of $\varepsilon_{i,j,k}$ over the entire forest.

Selected values of $\varepsilon_{i,j,k}$ are assembled in Figure 3 as contour plots of the snow surface. The plots show the general shape of the snow surface from the last observation of each field season between 1990 and 1995. From this figure it is apparent that snow does not accumulate uniformly on the surface of the ice sheet on this length scale. Rather, dunes and valleys exist with an amplitude less than 15 cm. Moreover, significant variation in the annual accumulation rate is detectable on spatial scales as low as 10 m. That is, a point on the surface of the grid that is below the mean elevation in one year may receive more snow than the average of the entire forest in the next year. It is also noteworthy that dunes on the snow surface do not persist from one year to the next.

The mean value of $\varepsilon_{i,j,k}$ is zero by definition since it is a measure of the deviation of the snow surface from a horizontal plane through the forest. Assuming that the variance of ε is stationary in time, it is reasonable to pool all of the observations of $\varepsilon_{i,j,k}$ in order to examine the frequency distribution of the snow surface deviation. Figure 4 shows the histogram of all of the calculated values of $\varepsilon_{i,j,k}$. The standard deviation of $\varepsilon_{i,j,k}$ on the 100 m x 100 m scale (denoted by σ_ε) is 4.5 cm. It should be emphasized that this value was obtained for summertime measurements only. A similar accumulation study at south pole found that the magnitude of σ_ε changes with season and is dependent on the local wind speed [*McConnell et al.*, 1997].

In addition, the frequency distribution has a skewness of 0.22 and a kurtosis of 0.20, both of which are greater than zero with more than 99% confidence. Physically, the positive skewness suggests that the dunes on the snow surface extend further above the median surface level than the valleys extend below the median surface. This is consistent with the shape of ocean waves in which the water forms smooth valleys and sharp crests. The positive kurtosis implies that the frequency distribution is more heavily weighted near the mean value compared to a normal distribution. That is, there are less dunes and valleys than would be expected if the snow surface were normally distributed.

The frequency distribution in Figure 4 was calculated for a single grid. It is likely that on other length scales the distribution will change. In particular, we might expect the value of σ_ε to vary directly with the distance between measurement points. The dependence of σ_ε on area will not be examined here. However, the value of 4.5 cm will probably be different on grids with different sizes and in

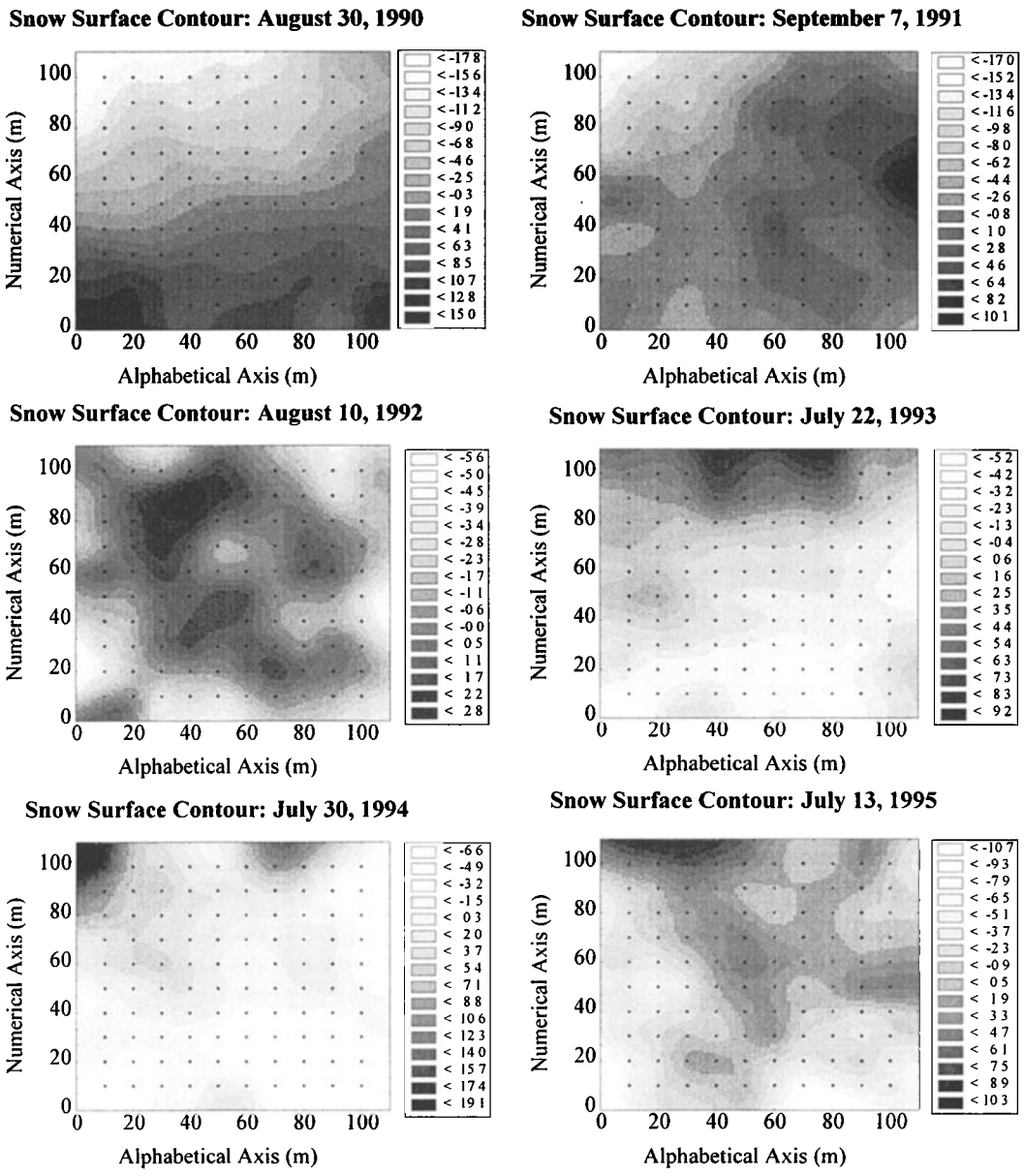

Figure 3. Snow surface contours for the ATM bamboo forest at the end of the summer field seasons from 1990 to 1995. Plots show that snow accumulates in a spatially non uniform way. The legends indicate the deviation of the surface from a horizontal plane in centimeters.

regions with different annual accumulation [*Fisher et al.*, 1985].

3.2. Correlation Regression

In the following analysis, the signal-to-noise variance ratio developed by *Reeh et al.* [1977] and *Fisher et al.* [1985] is expanded to apply to a larger range of spatial and temporal scales. Using the notation of these authors, the accumulation rate λ is defined as the time derivative of the accumulation A.

$$\lambda(i) = \frac{dA_i(t)}{dt} \quad (4)$$

Multiple observations of the value of $\lambda(i)$ at a fixed interval Δt produce a vector of the accumulation rates at location i. This vector is composed of two components: a regionally homogeneous signal term S and a spatial noise term e_i.

$$\lambda(i) = S + e_i \quad (5)$$

The S component is the accumulation signal shared by all ice cores within the defined region, while the e_i component is the noise that is unique for each individual ice core. For the purpose of investigating changes in the accumulation over a large area, we are interested only in S. Thus the term e_i interferes with our ability to infer regional climatic information from a single ice core signal.

Fisher et al. [1985] have shown that it is possible to estimate the relative contribution of S and e_i from a pair of ice core signals. The ratio of the signal variance to the noise variance F can be inferred from the correlation coefficient between the accumulation records from two parallel ice cores $r_{\lambda(i),\lambda(j)}$.

$$F = \frac{\mathrm{var}[S]}{\mathrm{var}[e_i]} = \frac{r_{\lambda(i),\lambda(j)}}{1 - r_{\lambda(i),\lambda(j)}} \quad (6)$$

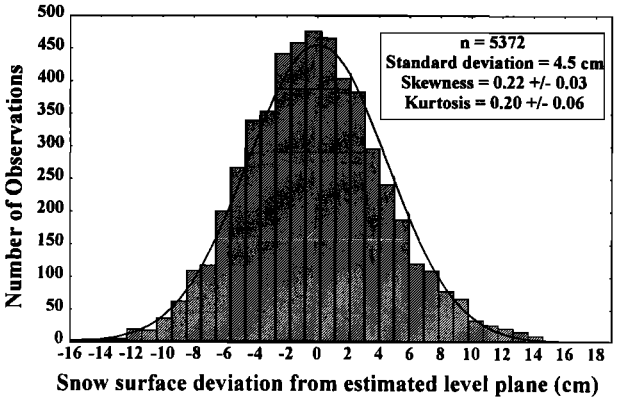

Figure 4. Histogram of the vertical distribution of snow levels derived from the 100 pole bamboo forest. The uncertainties associated with the skewness and kurtosis are the standard errors. The solid line is the normal distribution of the snow surface deviation with a mean of 0 and standard deviation of 4.5 cm.

Note that the correlation coefficient between two ice cores $r_{\lambda(i),\lambda(j)}$ is equivalent to the squared correlation coefficient between an ice core and the regional accumulation signal $r^2_{\lambda(i),S}$. Qualitatively, if two ice cores taken some distance Δx apart are highly correlated ($r_{\lambda(i),\lambda(j)} \rightarrow 1$), then the variance of the regional signal S dominates over the noise signal e_i ($F \rightarrow \infty$). Conversely, if F is low, then the ice core record is not representative of the regional accumulation signal and interpretation of this signal on the given timescale is not meaningful. It should be noted that the signal-to-noise variance ratio is different than the signal-to-noise ratio. The signal-to-noise ratio is defined as the amplitude of the signal divided by the amplitude of the noise.

Figure 5 illustrates examples of signals that are frequently encountered in ice core records: a sinusoidal oscillation, a sudden event, and a shift from one constant value to another. The scale in this figure was chosen so that the variance of each signal of 20 points was equal to 1. A series of normally distributed random numbers were added to each signal such

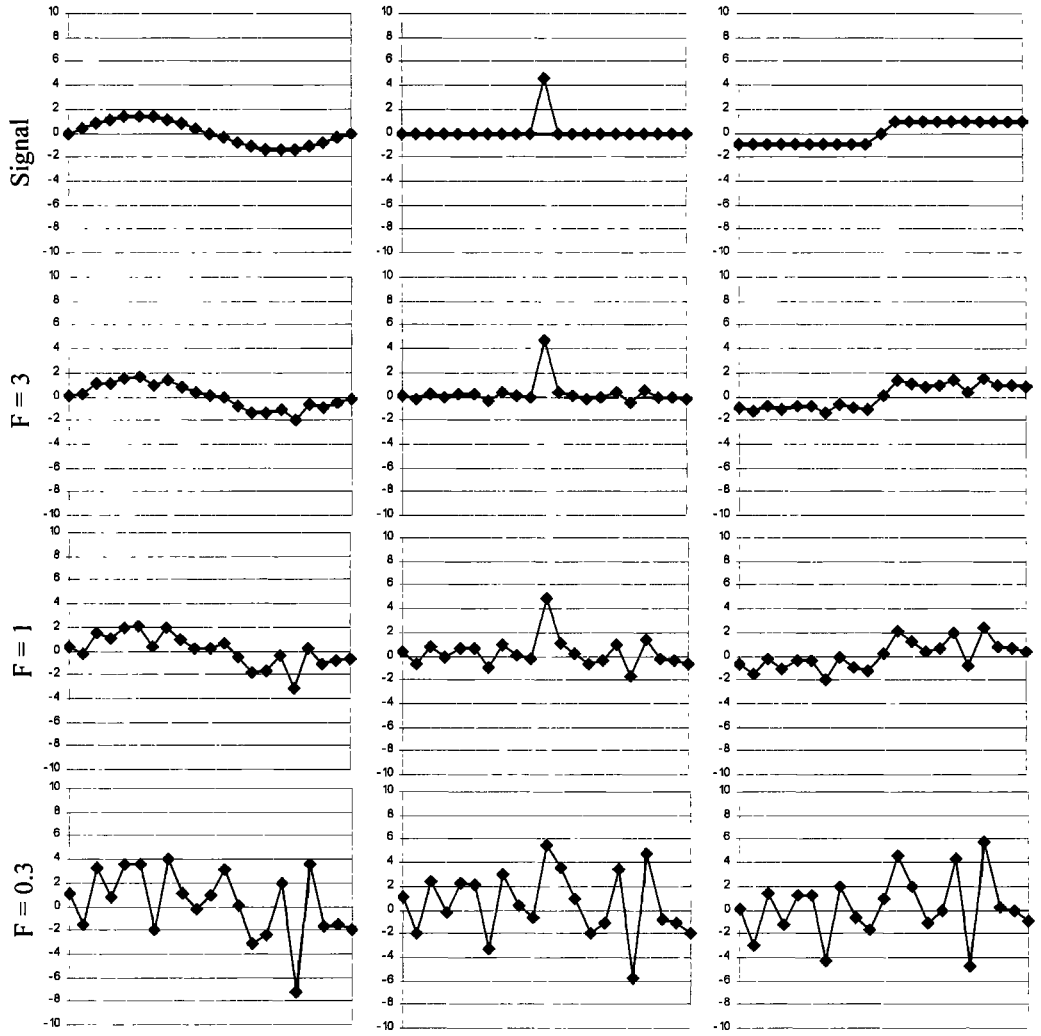

Figure 5: Examples of signals with different signal-to-noise variance ratios: (left) sine, (middle) event, and (right) shift.

that the resulting signal-to-noise variance ratio corresponds to the labels on the left side of the figure. For this example, at F = 1 and below, it is difficult to discern the patterns of both the sinusoid and the shift, and at F = 0.3 the event is no longer distinguishable from neighboring data points.

3.3. Dependence of F on Temporal Sampling Interval Δt

The forest data set contains a wealth of accumulation information on different temporal and spatial scales. From the 59 dates that the forest measurements were taken, pairs of dates have been selected that span one of three time intervals Δt: 1 week (6 to 8 days), 1 month (25 to 35 days), and 1 year (346 to 357 days). A total of 15 pairs have been selected with Δt = 1 week, 12 pairs were selected with Δt = 1 month, and 5 pairs were selected with Δt = 1 year. For each bamboo pole i the net snow accumulation between each pair of dates was calculated. From these accumulation time series $\lambda(i)$ a correlation matrix was constructed for every pair of $\lambda(i)$ in the forest. Thus for each interval Δt, there were ~5000 realizations of the correlation coefficient $r_{\lambda(i),\lambda(j)}$ corresponding to each pair of bamboo poles. The mean value of the correlation coefficients $\bar{r}_{\lambda(i),\lambda(j)}$ and the standard error of $r_{\lambda(i),\lambda(j)}$ (the standard deviation of the observations divided by the square root of the number of observations) were then calculated from the ~5000 realizations. This analysis was repeated for each interval Δt. The top panel of Figure 6

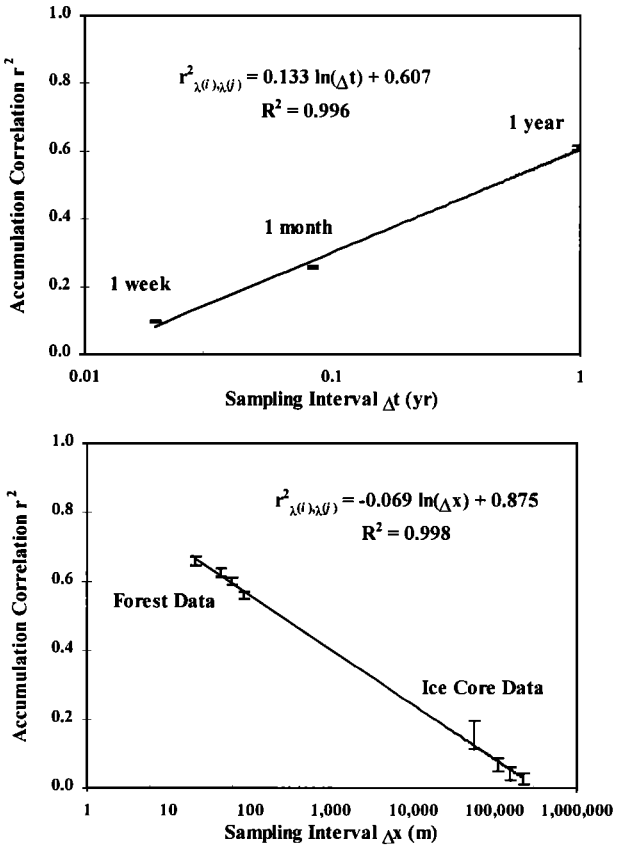

Figure 6. Regressions of the accumulation correlation r2 values versus time interval of ice core samples and distance between cores. (top) Accumulation data collected at the bamboo forest, and (bottom) combination of the forest data with data from ice core surveys [*Bolzan and Strobel*, 1994; *Clausen et al.*, 1988].

shows the results of the regression of the square of the average value of correlation coefficients calculated from the entire forest $\bar{r}^2_{\lambda(i),\lambda(j)}$ versus the logarithm of each value of Δt. The figure shows that the correlation between two ice core accumulation records improves as the time interval Δt increases. Since there are approximately ~5000 realizations of $r_{\lambda(i),\lambda(j)}$, the standard errors of $r_{\lambda(i),\lambda(j)}$ are quite small. While Figure 6 only shows the relationship between $\bar{r}^2_{\lambda(i),\lambda(j)}$ and Δt, given $\bar{r}^2_{\lambda(i),\lambda(j)}$, one can calculate the signal-to-noise variance ratio F by first calculating $\bar{r}_{\lambda(i),\lambda(j)}$ and applying the result to equation 6.

The choice of a logarithmic relationship between $\bar{r}^2_{\lambda(i),\lambda(j)}$ and Δt is somewhat arbitrary. Of the four types of relationships tested (linear, logarithmic, power, and exponential), the logarithmic relationship was chosen because the R^2 of the regression was highest. (Note the difference in notation for the correlation coefficient r. A lowercase r is used to refer to the correlation of two accumulation records. An uppercase R refers to the correlation between observed values and modeled values.)

3.4. Dependence of F on Spatial Distance Between Accumulation Records

A comparable analysis has been performed relating the horizontal spacing between individual accumulation records and the signal-to-noise variance ratio. To analyze the effect of spatial separation on F, only accumulation records with Δt = 1 year were considered.

The distance between poles in the forest ranges between 10 m for adjacent poles and 127 m for the pairs of poles on the corners of the grid. The 5000 distances between all of the pairs of poles were separated into four roughly equal size groups of ~1250 based on size. That is, the lower 25% of the distances were in the range 10 - 32 m (geometric mean 21 m), the distances between the 25 and 50 percentiles spanned 33 - 50 m (geometric mean 43 m), the distances between the 50 and 75 percentiles spanned 50.5 - 70 m (geometric mean 59), and the upper 25% had distances in the range 70.5 - 121 m (geometric mean 83 m). The geometric mean of the distance was chosen instead of the arithmetic mean since the geometric mean values occur at the center of each cluster when plotted on a logarithmic scale. For each of these groups $\bar{r}^2_{\lambda(i),\lambda(j)}$ was calculated along with the standard error of $\bar{r}^2_{\lambda(i),\lambda(j)}$. These are the four data points in the upper left corner of the bottom panel of Figure 6. The $\bar{r}^2_{\lambda(i),\lambda(j)}$ value is plotted against Δx in this figure because the fit of the regression line is better than the regression lines for either $r_{\lambda(i),\lambda(j)}$ versus Δx or F versus Δx. The large number of correlation coefficients were reduced to four quartiles for presentation purposes. Individual values of $r_{\lambda(i),\lambda(j)}$ from the forest ranged from ~-1 to1 because a relatively small number of points (five for Δt = 1 year) were used. By presenting the mean and standard error for each quartile, the dependence of $\bar{r}^2_{\lambda(i),\lambda(j)}$ on Δx can be readily seen in the plot.

Since the Δx values from the forest were relatively small, additional shallow ice core data were incorporated into the database to expand the range of distances. Accumulation in the bamboo forest was measured in terms of a velocity (cm yr^{-1}), while accumulation from ice cores was typically measured as a mass flux (kg m^{-2} yr^{-1}). Since snow density was not measured at the bamboo forest, it was not possible to make a direct comparison of the two types of data sets. For

the sake of merging the two data sets in the following analysis, it is assumed that snow density is spatially uniform such that the forest accumulation measurements are a good approximation of the mass flux of snow to the ice sheet. Under this assumption, it is valid to compare the dimensionless correlation coefficients $\bar{r}^2_{\lambda(i),\lambda(j)}$ obtained from each of the data sets.

Bolzan and Strobel [1994] collected nine shallow cores from the Summit region spanning 22-41 years of accumulation through 1986. Data from this study were obtained via personal communication with John Bolzan. *Clausen et al.* [1988] also collected a series of eight ice cores in the vicinity of Crete, Greenland (71.12°N, 37.32°W, 3172 m asl) which is approximately 130 km to the south of Summit. The Clausen cores spanned 40 to 350 years through 1983. The accumulation data for the Clausen ice cores were obtained from the National Oceanic and Atmospheric Administration (NOAA) Paleoclimatology Program archive on the world wide web (NOAA Paleoclimatology Program-Ice Core Data Sets, http://www.ngdc.noaa.gov/paleo/ice-data.html, December 15, 1996). Snow accumulation records were obtained in ice equivalent cm yr^{-1} from each of the cores by measuring the distance between the minimums of the $\delta^{18}O$ annual cycle. In order to homogenize the combined data set, only the accumulation records spanning 1964 to 1983 were considered.

Using these 17 accumulation records, 136 realizations of $r_{\lambda(i),\lambda(j)}$ were calculated with Δt = 1 year. As with the forest data, all of the pairs of ice cores were grouped into quartiles based on distance between the coring sites. The range of distances was 18 to 278 km. The geometric mean distances of the ice core quartiles were 57, 111, 155, and 221 km. The $\bar{r}^2_{\lambda(i),\lambda(j)}$ values for each ice core spacing quartile are plotted in the lower right corner of the bottom panel of Figure 6.

The logarithmic regression of $\bar{r}^2_{\lambda(i),\lambda(j)}$ and Δx is presented in the bottom part of Figure 6. The trend line seems to fit both the forest and ice core values very well. While there is a considerable range of length scales between the forest data and the ice core data, the quality of the fit suggests that the trend line should be representative of the distances that fall between the two data sets.

The decreasing trend observed in Figure 6 is intuitive since one would expect cores collected with large spacing to have a smaller correlation than those collected at short distances. The figures indicate that the signal correlation between ice cores weakens with the logarithm of the spacing between the cores and that the trend is consistent over 4 orders of magnitude from 20 m to 200 km.

The two regressions in Figure 6 strongly indicate that the signal-to-noise variance ratio is a function of both the temporal interval Δt of each measurement within an accumulation data series, and the horizontal spacing between two sampling sites Δx. Based on the regressions used in Figure 6, it is proposed that the relationship between $\bar{r}^2_{\lambda(i),\lambda(j)}$, Δt, and Δx has the following form:

$$\bar{r}^2_{\lambda(i),\lambda(j)} = f(\Delta x)g(\Delta t) = \alpha(1+\beta\ln(\Delta x))(1+\gamma\ln(\Delta t)) \quad (7)$$

The multiplicative combination of the spatial correlation function and the temporal correlation function was initially proposed by *Rodriguez-Iturbe and Mejia* [1974] for use with rainfall measurements. Equation (7) has the advantage that the parameters α, β, and γ can be estimated using least squares linear regression techniques. In order to estimate the parameters, a data set was compiled using both the forest data and the ice core accumulation records from *Bolzan and Strobel* [1994] and *Clausen et al.* [1988]. From the forest, 12 values of $\bar{r}^2_{\lambda(i),\lambda(j)}$ were obtained from the mean correlation coefficients at the four quartile geometric mean distances Δx with accumulation intervals Δt of 1 week, 1 month, and 1 year. From the shallow ice cores, eight values of $\bar{r}^2_{\lambda(i),\lambda(j)}$ were calculated using the four quartile distances and Δt = 1 and 2 years.

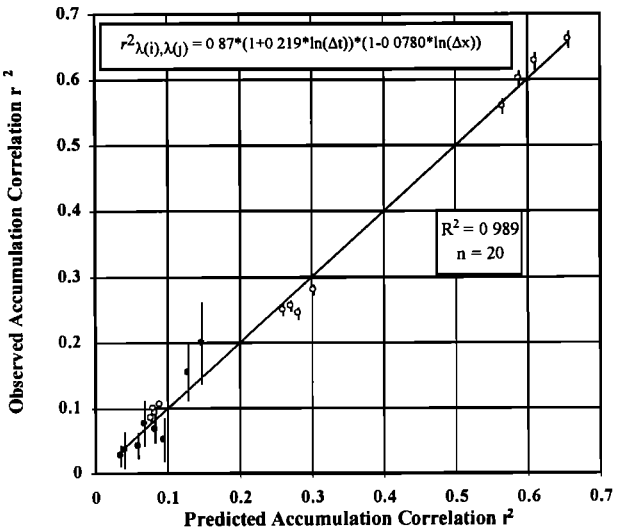

Figure 7. Observed versus predicted accumulation correlation coefficients. The error bars represent the standard error of r^2 calculated by propagating the standard error of r. The solid circles are the data points obtained from the Clausen et al. [1988] and Bolzan and Strobel [1994] ice cores. The open circles are the data points obtained from the bamboo forest data set.

Figure 7 shows the regression of the observed $\bar{r}^2_{\lambda(i),\lambda(j)}$ versus predicted values which are only a function of Δx and Δt. The error bars for the observed values in Figure 7 are calculated from the standard errors of $r_{\lambda(i),\lambda(j)}$. The parameters of the regression and their standard errors are

$$\bar{r}^2_{\lambda(i),\lambda(j)} = (0.87 \pm 0.02)(1-(0.0780 \pm 0.0008)\ln(\Delta x))(1+(0.219 \pm 0.004)\ln(\Delta t)) \quad (8)$$

where Δx is in meters and Δt is in years. While the parameters in the regression are purely empirical, the strong correlation in Figure 7 gives confidence that the signal-to-noise variance ratio for ice core accumulation records can be inferred with reasonable accuracy on the spatial and temporal scales of these experiments.

It should be emphasized that the model has been calibrated using Δx as the geometric mean of the spatial separation of all pairs of accumulation records. It would be useful to know how representative a single accumulation record is for a given area. Inferring the size of this area from Δx is problematic since Δx is a function of the number of records obtained from a given area and their spacing. For example, a coring traverse such as the one completed on the Expédition Glaciologique

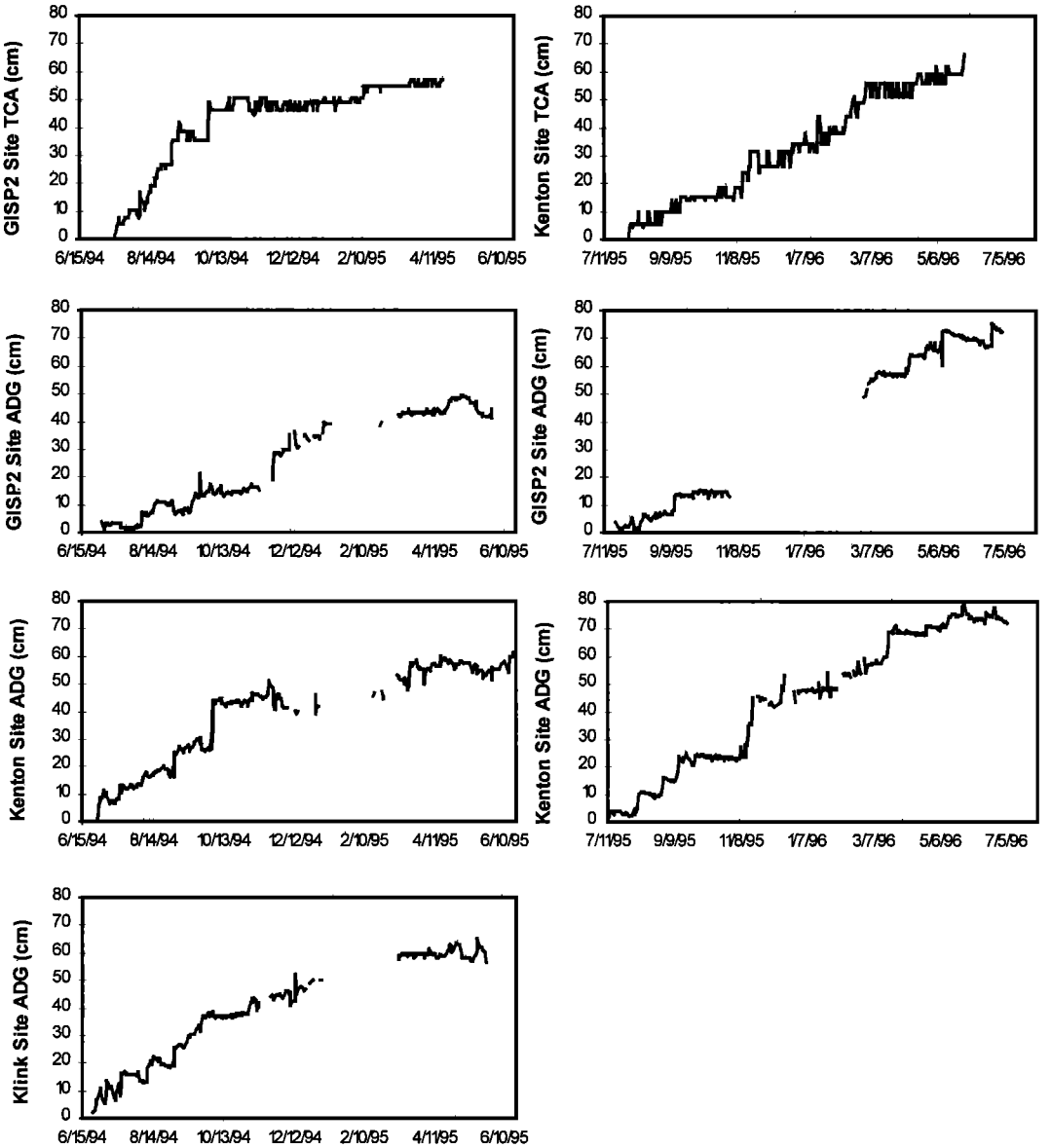

Figure 8. Winterover accumulation results from acoustic depth gauges and thermocouple array from GISP2, ATM (Kenton), and Klink sites on the Greenland Crest.

Internationale au Groenland (EGIG) line [*Fischer and Wagenbach,* 1996] would by definition span no area. However, the group of cores would have a geometric mean spacing Δx. In contrast, the nine Bolzan ice cores were arranged in a circular pattern and span an area of approximately 30,000 km^2. Thus these two experiments span different sized areas.

3.5. Acoustic Depth Gauges and Thermocouple Array

By using the correlation model (equation (8)) we can evaluate the array of automated accumulation monitors to determine if it is possible to resolve seasonal signals from these data. The daily average results of the winterover accumulation monitors are presented in Figure 8. The time series from the thermocouple array appears rougher than for the ADGs due to the discrete nature of the data collection process. The results show that snow does not accumulate simultaneously at each of the monitors.

The ADGs and TCA were initially installed near Summit to measure the seasonal variability of accumulation. To resolve a seasonal cycle of snow accumulation, Δt = 1 month would provide adequate resolution. One month accumulation signals were calculated from the ADGs and TCA. By correlating the monthly accumulation rate at each pair of monitors and taking the average of the correlation coefficients from all pairs, the result is $r_{\lambda(i),\lambda(j)} = 0.15 \pm 0.20$ where the uncertainty is the standard error of the nine correlation coefficients.

The geometric mean distance between the monitors Δx over the 2 years of deployment is 11 km. For these conditions, (8) predicts $\bar{r}_{\lambda(i),\lambda(j)} = 0.32$ which is in agreement with the observed values.

There are insufficient data from the ADG records to attempt this analysis using Δt = 3 months (i.e., there are too few data points for meaningful correlations). Nonetheless, (8) would predict $r_{\lambda(i),\lambda(j)} = 0.41$ and $F = 0.78$ which is still more

noise variance than signal variance. Consequently, it is impossible to use these automated accumulation experiments to infer the seasonal variability of snow accumulation over the region where they were deployed.

3.6. Useful Applications of the Regression

It is possible to determine how many ice cores would be needed to accurately resolve accumulation records on shorter timescales for any given Δx. If we take the average of a series of accumulation records, then the standard error of the mean is inversely proportional to square root of the number of records averaged. Thus for a series of n cores the average signal has a higher signal-to-noise variance ratio by a factor of n. If we define F_{target} as the signal-to-noise variance ratio of the averaged signal, then it can be shown that

$$n = \frac{F_{\text{target}}}{F(\Delta x, \Delta t)} \qquad (9)$$

This equation along with (6) and (8) can in turn be used for experimental design to determine how many cores are necessary to resolve the accumulation record on a given timescale. For annual accumulation Δt = 1 year, with a length scale of Δx = 100 km and F_{target} = 3, the result of this calculation is approximately 7 cores.

Concerning the ADG experiment, in order to resolve a seasonal accumulation trend (i.e., Δt = 1 month, Δx = 1 km, and F_{target} = 3), it would be necessary to deploy at least six monitors. Longer records would also be needed to ensure accurate measurements of $r_{\lambda(i),\lambda(j)}$. To obtain the seasonal accumulation signal over the larger Summit - Crete region, many more monitors would need to be deployed.

3.7. Central Greenland Accumulation Trends (1964 to 1983)

Given that multiple cores are needed to improve the signal-to-noise variance ratio, the accumulation records from *Clausen et al.* [1988] and *Bolzan and Strobel* [1994] have been compiled in an attempt to extract a regional accumulation signal for the period 1964 to 1983. Since the average annual accumulation over the 20 year period varies depending on the site from 17.8 to 36.5 cm ice equivalent yr^{-1}, it is necessary to normalize each accumulation record with respect to its accumulation mean and standard deviation over the interval before averaging each of the records. The normalized accumulation signal is defined as

$$I_i = \frac{\lambda(i) - \overline{\lambda(i)}}{\sigma_{\lambda(i)}} \qquad (10)$$

In this way the signal I_i from each ice core i has a mean of 0 and standard deviation of 1 over the 20 year interval. Figure 9 shows the average normalized accumulation signal $\bar{I}$ from 1966 to 1983. That is, for each year, $\bar{I}$ is the average of all values of I_i. The error bars in the figure are the standard errors of I_i from the 17 cores. Of the 20 years in the series, 9 were significantly different than the mean with >99% confidence (i.e., the absolute difference between $\bar{I}$ and 0 was greater than 3 times the standard error of $\bar{I}$ for that year).

Bromwich et al [1993] compared modeled precipitation rates from meteorological records with an ice core record from the Dye 3 site [*Reeh et al.*, 1977]. The comparison showed that some features of the accumulation records were consistent on an interannual basis although the correlation was not strong. Using an accumulation record with a larger signal-to-noise variance ratio such as $\bar{I}$ in Figure 9 may yield better agreement between the observed and predicted accumulation records.

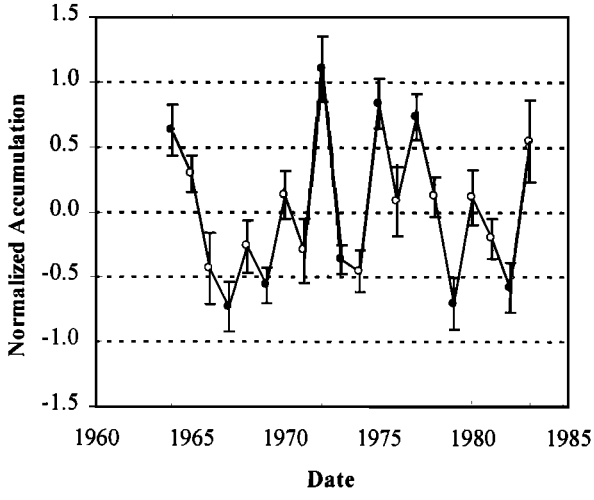

Figure 9. Normalized accumulation signal from central Greenland between 1966 and 1983. The error bars are the standard error of the average normalized accumulation from the 17 ice core collected from the Bolzan survey [*Bolzan and Strobel*, 1994] and the Clausen survey [*Clausen et al.*, 1988]. The locations of these cores are shown in Figure 1. The solid circles are years where the snow accumulation was different from the mean annual accumulation with greater than 99% confidence.

Bolzan and Strobel [1994] performed a similar analysis on the same series of ice core records. Rather than normalizing each record, these authors combined the accumulation records to estimate the total accumulation of snow over the survey grid. Their record more closely approximates the net flux of snow to the region, while the normalized accumulation record $\bar{I}$ approximates the average accumulation signal shared by all of the cores.

3.8. Alternative Methods for Calculating the Signal-to-Noise Variance Ratio F

The signal-to-noise variance ratio for the accumulation index can be calculated directly by two methods. The first is to calculate the mean correlation coefficient of the 136 pairs of accumulation records and obtain F from (6). Since $\bar{I}$ is the average of 17 cores, the signal-to-noise variance ratio should be multiplied by 17 as in (9). The result of this calculation yields $F_I = 5.8 \pm 0.5$.

The second method is to directly calculate the ratio using the mean and standard error values of the accumulation index. The variance of $\bar{I}$ over the 20 year interval is the sum of the signal and noise variances. The standard error of I_i for each year is the square root of the yearly noise variance var[e]. Hence F_I can be calculated as

$$F = \frac{\text{var}[S+e] - \text{var}[e]}{\text{var}[e]} \qquad (11)$$

The result of this calculation is F_I = 6.2 which by the definition of F is in agreement with the previous method.

Finally, (8) and (9) can be tested against the combined ice core data set. Using the geometric mean of the distance between the cores $\Delta x = 121$ km, $\Delta t = 1$ year, and $n = 17$ cores, the modeled signal-to-noise variance ratio calculated from (6), (8), and (9) is $F_I = 6.4 \pm 0.2$ which is also in agreement with the direct calculation methods above. The uncertainty of the modeled estimate is based on the propagation of the standard errors of the parameters α, β, and γ in (8). The general agreement between the model and observed values is not surprising since the model was calibrated using data from these 17 cores.

The spatial applicability of the model is limited by the area over which the signal can reasonably be considered to be homogeneous. In reality, the regional signal will be inhomogeneous to some extent, no matter what spatial scale is considered. Additional studies similar to this one will be necessary to infer signal-to-noise variance ratios for accumulation records in other parts of the world.

4. Conclusions

Snow accumulation records spanning 6 years from a set of 100 bamboo poles in a 90 m x 90 m area have been analyzed to estimate the spatial and temporal variability of snow accumulation near Summit, Greenland. Using a numerical optimization technique, contours of the snow surface within the area have been estimated. The results suggest that the deviation of the snow surface from a horizontal plane is approximately normally distributed with a small but significant amount of positive skewness and kurtosis.

Data from the bamboo poles have been merged with accumulation records from shallow ice cores to construct a spatial-temporal noise model. Given a specified sampling interval (1 week $< \Delta t <$ 2 years) and length scale (20 m $< \Delta x <$ 200 km), the parameters of the regression can be used to estimate the signal-to-noise variance ratio of a given accumulation record. The analysis suggests that for the annual accumulation signal in central Greenland for cores spaced 100 km apart, the signal-to-noise variance ratio F is 0.42. Given the accumulation records of multiple ice cores, it is possible to obtain a regional accumulation record with a higher signal-to-noise variance ratio. Also, when the sampling interval within an ice core is increased, the noise variance is reduced, and significant trends representing regional accumulation emerge from the record. The noise model and automated measurements indicate that no seasonal variation in the accumulation record can be detected using four accumulation monitors with geometric mean spacing of ~11 km.

A regional average accumulation signal has been calculated from 17 shallow cores collected in the Summit-Crete region. The signal-to-noise variance ratio for the 20 year record spanning 1964 to 1983 is ~ 5.8. This regional signal will be useful to climate modelers attempting to match general circulation model output with ice core accumulation records in the Summit region.

Acknowledgments. We would like to thank MattPender, Valerie Hart, Jim Winterle, and François Lapierre for their assistance in the field and John Bolzan for contributing ice core accumulation data. Dietmar Wagenbach assisted with ideas on the thermocouple array. We would also like to thank the Polar Ice Coring Office and the New York Air National Guard 109th TAG for logistic support in Greenland, and the Danish Research Commission for allowing us the opportunity to work at Summit. This work was supported by NSF grants OPP-9222963, OPP-9321642, OPP-9423410, and OPP-9530670. The European participants were funded by the EC under the grant EV5V-0412 (program TAGGSI).

References

Bolzan, J. F., and M. Strobel, Accumulation rate variations around Summit, Greenland, *J. Glaciol., 40*, 56-66, 1994.

Bromwich, D. H., F. M. Robasky, R. A. Keen, and J. F. Bolzan, Modeled variations of precipitation over the Greenland Ice Sheet, *J. Clim., 6*, 1253-1268, 1993.

Clausen, H. B., N. S Gundestrup, S. J. Johnsen, R. Bindschadler, and J Zwally, Glaciological investigations in the Crête area, Central Greenland: A search for a new deep-drilling site, *Ann. Glaciol., 10*, 10-15, 1988.

Dibb, J. E., and J.L Jaffrezo, Air-snow exchange investigations at Summit, Greenland: An overview, *J. Geophys. Res* in press, 1997.

Fischer, H., and D. Wagenbach, Large-scale spatial trends in recent firn chemistry along an east-west transect through central Greenland, *Atmos. Environ., 19*, 3227-3238, 1996.

Fisher, D. A., N. Reeh, and H. B. Clausen, Stratographic noise in time series derived from ice cores. *Ann. Glaciol., 7*, 76-83, 1985.

Jaffrezo, J. L., J. E. Dibb, R. C. Bales, and A. Neftel, Current status of atmospheric studies at Summit (Greenland) and implications for future research, in *Ice Core Studies of Global Biogeochemical Cycles, NATO ASI Ser 1., 30*, edited by R. J. Delmas, 428-458, 1995

Mayewski, P., M. Spencer, M. Twickler, and S. Whitlow, A glaciochemical survey of the Summit region, Greenland, *Ann Glaciol., 14*, 186-190, 1990.

McConnell, J , R. Bales, and D. Davis, Recent Intra-annual snow accumulation at south pole: Implications for ice core interpretation,*J Geophys. Res , 102*, 21,947-21,954, 1997.

Palais, J., Snow stratigraphic investigations at Dome C, East Antarctica : a study of depositional and diagenetic processes, M.S. thesis, 146 pp., Ohio State Univ., Columbus, 1980.

Reeh, N.. H. B Clausen, N. Gundestrup, S. J. Johnsen, and B. Stauffer, $\delta(^{18}O)$ and accumulation rate distribution in the Dye 3 area, south Greenland, *IAHS Publ., 118* , 177-181, 1977.

Rodriguez-Iturbe, I., and J. M. Mejia, On the transformation of point rainfall to areal rainfall, *Water Resour Res., 10*, 729-735, 1974.

M. Bergin, NOAA, CMDL, R/E/CG1, Boulder, CO 80303 (email: mbergin@cmdl.noaa.gov)

C. Davidson, Department of Civil and Environmental Engineering, Carnegie Mellon University, Pittsburgh, PA 15213 (email: cliff@andrew.cmu.edu)

J. Dibb, Glacier Research Group, Institute for the Study of Earth, Oceans, and Space, University of New Hampshire, Durham, NH 03824 (email: Jack_Dibb@grg.sr.unh.edu)

H. Kuhns, Energy and Environmental Engineering Center, Desert Research Institute, Las Vegas, NV 89119 (email: hkuhns@snsc.dri.edu)

C. Stearns, Department of Atmospheric and Oceanic Sciences, University of Wisconsin, Madison, WI 53706 (email: chucks@ssec.wisc.edu)

(Received February 20, 1997; revised September 22, 1997; accepted September 25, 1997.)